Electronic Supplementary Material (ESI) for Nanoscale.

Probing the Plasmon-Driven Suzuki-Miyaura Coupling Reactions with Cargo-TERS towards Tailored Catalyzation

*Zhandong Li[1], and Dmitry Kurouski[*1,2]*

[1]Department of Biochemistry and Biophysics, Texas A&M University, College Station, Texas 77843, United States

[2]The Institute for Quantum Science and Engineering, Texas A&M University, College Station, Texas, 77843, United States

Content:

References

Experimental details

1. Chemicals

Gold (III) chloride trihydrate ($HAuCl_4 \cdot 3H_2O$, 99.9%), palladium (II) chloride solution (H_2PdCl_4), hexadecyltrimethylammonium bromide (CTAB, 99%), 4-Mercaptophenylboronic acid (4-MPBA), 4-Fluoro-(Chloro- and Bromo-) thiophenol (4-FTP, 4-CTP and 4-BTP), sodium hydroxide (NaOH, 98%), potassium iodide (KI, 99%), L-ascorbic acid (AA, 99%), and sodium borohydride ($NaBH_4$, 99%) were purchased from Sigma-Aldrich (St. Louis, MO). Sodium citrate dihydrate (Na-Cit, 99%) was purchased from Fisher scientific (Waltham, MA). Ethanol was purchased from Decon Labs (King of Prussia, PA). All chemicals were used as received without purification.

2. Sample preparation

For preparing Au@PdNPs, a three-step synthetic approach[1] was employed (Fig. S1). At the first step, seed-mediated growth of thin AuNPs (15 nm) was performed; at the second step, isotropical growth 15 nm AuNPs to 70 nm AuNPs was made; lastly, exposition of 70 nm AuNPs to Pd ions for deposition of sub-monolayer of Pd nanostructures on the surface of AuNPs was done. For seed-mediate growth, Au nanoparticle seeds were prepared by mixing $HAuCl_4$ solution (0.01 M, 2 mL), Na-Cit (0.01 M, 1 mL) and 36 mL of water. Then, freshly prepared ice-cold $NaBH_4$ (0.1 M, 1 mL) was mixed the above solution under vigorous stirring for 2 min. After aging at room temperature for over 2 h, the Au seed solution will be ready for using for next step. Three bottles of growing solutions were prepared separately in three flasks. The first two solutions were prepared following the same recipe, CTAB (0.05 M, 9 mL) solution was prepared separately in two flasks and then $HAuCl_4$ (0.01 M, 0.25 mL) solution, NaOH (0.1 M, 0.05 mL) solution, KI (0.01 M, 0.05 mL) solution, and ascorbic acid (AA, 0.1 M, 0.05 mL) was added into the two flasks by order. The third growing solution was prepared in a tenfold larger quantity than the first two growing solutions. Similarly, $HAuCl_4$ (0.01 M, 2.5 mL) solution, NaOH (0.1 M, 0.5 mL) solution, KI (0.01 M, 0.5 mL) solution, and AA (0.1 M, 0.5 mL) solution was added into CTAB solution (0.05 M, 90 mL). Then 1 mL of the as-prepared Au seeds solution was added into the first growing solution with gently shaking for 5 s. Subsequently, 1 mL of the mixture of the above-mentioned solution was added to the second growth solution, followed by a gently shaking for another 5 s. Then, all of the mixture of Au seeds and growth first and second solutions was added to third growing solution and shake for 5 s. The final solution was then

kept at room temperature for over 12 h without further disturb. Then, after centrifuge, the supernatant was removed, the thin AuNPs (15 nm) were re-dispersed and collected by centrifuging at 5000 rpm for 2 min and re-dispersed in CTAB solution (5 mL, 0.1 M) serving as seeds for isotropic growth of thick AuNPs next. Thick AuNPs (70 nm) were prepared by isotropic growth in a diluted CTAB (0.01 M) solution. The growth solution was prepared as following, $HAuCl_4$ (0.25 M, 1 mL) solution, AA (0.1 M, 0.055 mL) solution, water (8 mL) and CTAB (0.1 M, 1 mL) solution was added by order in the flask followed by gently shaking. Then, a solution contacting thin AuNPs seeds (0.25 mL,15 nm) was added to the growing solution to initialize the isotropic growth. Then, the thickness of the as-prepared AuNPs was at least 70 nm, which was determined using AFM. For bimetallic Au@PdNPs, according to the previous reported method,[1] AA (60 μL, 20 mM) solution was first added into the solution containing thick AuNPs (250 μL, 70 nm) and mixed by vortexing for 10 s. Subsequently, H_2PdCl_4 (15 μL, 10 mM) solution were added followed by vortexing for another 10 s. The above mixture was kept at room temperature for 1 h until the Pd layer formed on the top of AuNPs. The solution was then centrifuged twice for 2 min at 8000 rpm. Finally, after removal of the supernatant, the Au@PdNPs were re-dispersed in 1.0 mL of water and sonicated for over 20 s.

3. Modification of the chemical agents on AuNPs/Au@PdNP and TERS tips

A fresh silicon wafer was cut into small squares of about 5×5 mm each. After sonicating in acetone and ethanol, all the small wafers were dried by nitrogen gas before use. As-prepared AuNPs/Au@PdNPs in stock solution were then deposited onto the pre-cleaned Si wafer and kept at room temperature for 30 min, allowing for the adsorption of nanoparticles onto the surface. Next, the Si wafer with deposited nanoplates was immersed in a 2 mM 4-XTP (X=F, Cl or Br) or 4-MPBA solution for 1 h to form a monolayer of these molecules on surfaces of these nanoparticles via Au-S bond. The modified sample was then sonicated in ethanol for 5 min to remove the uncoordinated molecules. Au-coated TERS tips were directly immersed in 1 mM of above-mentioned molecules for half hour and rinsed with ethanol for thrice in ethanol before use.

4. Metal deposition on AFM tips.

Silicon AFM probes with Al on reflex side, force constant 2.0 N/m and resonance frequency 70 kHz were purchased from NanoAndMore USA Corporation (Watsonville, CA). For gold coating, in brief, ten sets of clamping devices were prepared for fixing the tips. Each device was then loaded with two tips and loaded into the thermal evaporator chamber (MBrown, Stratham, NH). Before the deposition start, the chamber

was allowed to evacuate to ~8×10-7 mbar. The inner pressure was kept at this pressure or below during the deposition. Then, with increasing heat, gold pellets (Kurt J. Lesker, Efferson Hills, PA) thermally melted and evaporated at constant 0.1-0.2 Å·s^{-1} rate. After 70 nm of Au was deposited on the AFM tips, the evaporation was stopped and kept cooling down to room temperature. The temperature at the tip surface and deposition chamber was ~50 °C.

5. Tip-Enhanced Raman Scattering (TERS) instrument set-up

AIST-NT-HORIBA system equipped with a 632.8 nm continuous wavelength (CW) laser was used for Atomic Force Microscopy (AFM) scanning experiments, AFM-TERS, and spectrum collections. Laser light was brought to the sample surface in a side-illumination configuration with a 100X Mitutoyo microscope objective. The scattered electromagnetic radiation was also collected with the same objective and directed into a fiber-coupled Horiba iHR550 spectrograph that is equipped with a Synapse EM-CCD camera (Horiba, Edison, NJ). The laser power throughout the TERS experiments was around 90 μW with 0.5 s acquisition time.

6. Scanning Electron Microscopy (SEM) characterization.

SEM characterization of AuNPs/Au@PdNPs was conducted on a JEOL scanning electron microscope (JSM-7500F).

7. DFT calculation.

DFT calculations. All calculations were performed using a development version of NWChem.[2] Unconstrained geometry optimization was performed using the PBE exchange-correlation functional[3] in conjunction with the def2-TZVP basis[4] set and a fitting basis[5] for the evaluation of the Coulomb potential. Ensemble-averaged Raman spectra and vibrational mode-dependent molecular polarizability derivatives were computed using the CPKS method, as implemented in NWChem.[2] Ensemble-averaged Raman scattering activities (*Sm*) are given by[6,7]

$$S_m = g_m[45\alpha_m'^2 + 7\beta_m'^2] \quad (1)$$

where

$$\alpha_m' = \frac{1}{3}(\tilde{\alpha}_{xx,m}' + \tilde{\alpha}_{yy,m}' + \tilde{\alpha}_{zz,m}') \quad (2)$$

and

$$\beta_m^{'2} = \frac{1}{2}[(\tilde{\alpha}_{xx,m}^{'} - \tilde{\alpha}_{yy,m}^{'})^2 + (\tilde{\alpha}_{yy,m}^{'} - \tilde{\alpha}_{zz,m}^{'})^2 + (\tilde{\alpha}_{zz,m}^{'} - \tilde{\alpha}_{xx,m}^{'})^2 + 6(\tilde{\alpha}_{xy,m}^{'2} + \tilde{\alpha}_{xz,m}^{'2} + \tilde{\alpha}_{yz,m}^{'2})] \quad (3)$$

In the above equations, g_m is the vibrational state degeneracy and primes denote derivatives with respect to the m^{th} state, $\alpha_m^{'}/\beta_m^{'2}$ are the isotropic/anisotropic polarizabilies, and $\tilde{\alpha}_{ij,m}^{'}$ (*i,j* = x,y,z) are components of the polarizability tensor.

The spectrum of an oriented molecule can be simulated according to:

$$S_n^2 \alpha \sum_n \left| \vec{E}_s^L R_z^T R_y^T R_x^T \tilde{\alpha}_n^{'} R_z R_y R_x \vec{E}_i^L \right|^2 \quad (4)$$

Here, molecular polarizability derivative tensor elements ($\tilde{\alpha}_n^{'}$) of a molecule are oriented with respect to the vector components of the local electric fields along incidence and scattering directions in the TER geometry ($\vec{E}_{i,s}^L = \vec{E}_z^L$) after (i) projection of the molecular onto the laboratory frame, and (ii) rotating the molecule (using rotation matrices $R_{x,y,z}$ and $R_{x,y,z}^T$). We will revisit this analysis in the ensuing sections of this work.

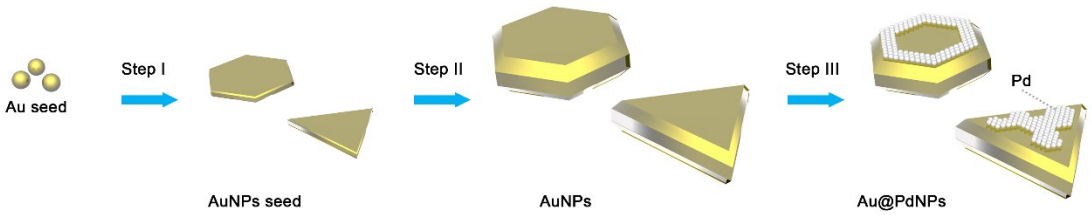

Fig. S1. Schematic illustration of three-step preparation of Au@PdNPs. At the step 1, seed mediated growth of 15-nm AuNPs was initiated; at the step II, isotropical growth of 70-nm AuNPs was performed; at the step III, a sub-monolayer of Pd on the top of AuNPs was made to yield Au@PdNPs.

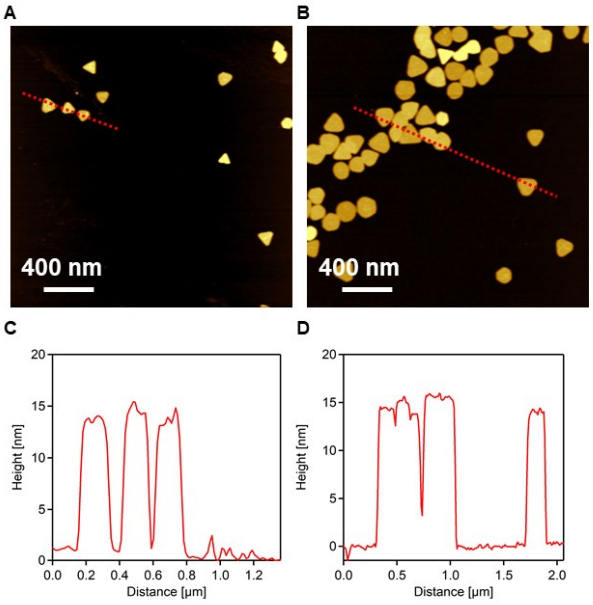

Fig. S2. AFM images and height profiles of thin AuNPs seed with ~15 nm in height. (A-B) AFM images of AuNPs. (C-D) Height profiles of AuNPs in (A-B).

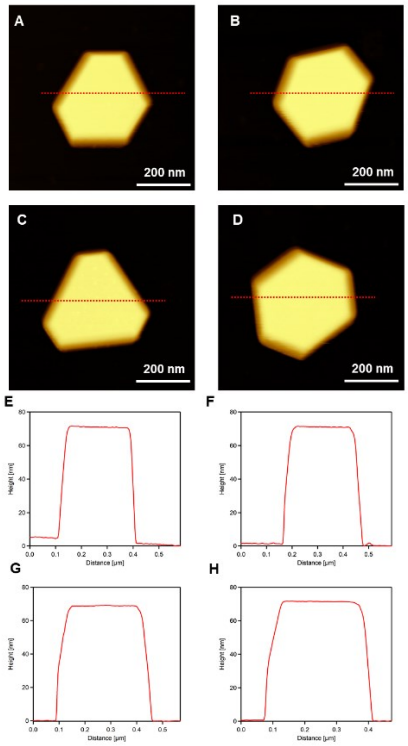

Fig. S3. AFM images and height profiles of thick AuNPs with ~70 nm in height. (A-D) AFM images of thick AuNPs. (E-H) Height profiles of AuNPs in (A-D).

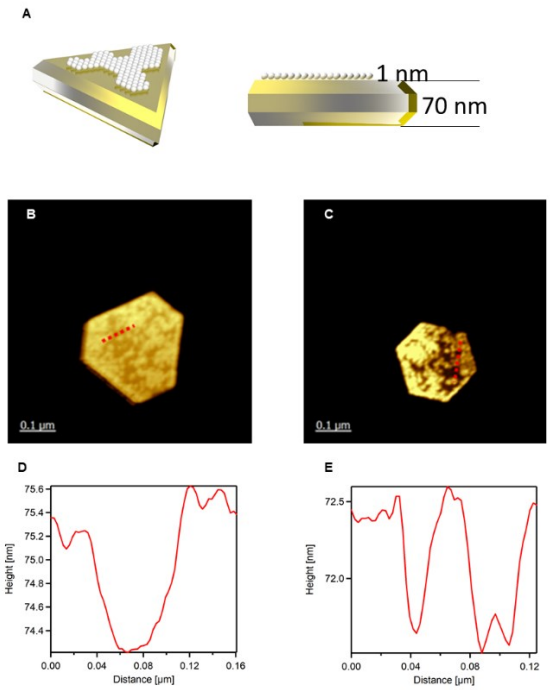

Fig. S4. (A) Schematic drawing of Au@PdNPs with ~1 nm of Pd layer on the surface of 70 nm Au. (B-C) AFM images of thick Au@PdNPs. (D-E) Height profiles of Au@PdNPs in (B-C).

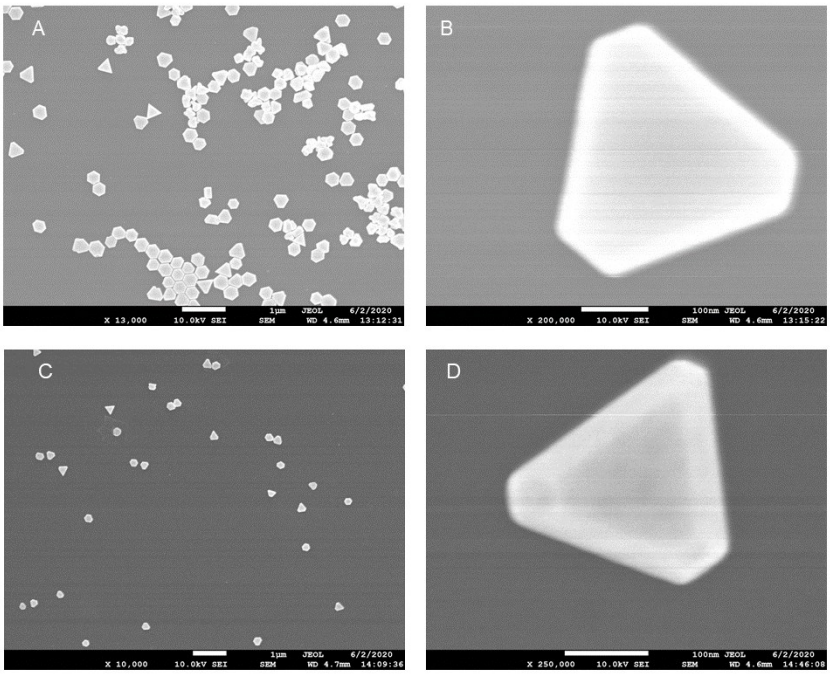

Fig. S5. SEM images of (A-B) AuNPs and (C-D) Au@PdNPs.

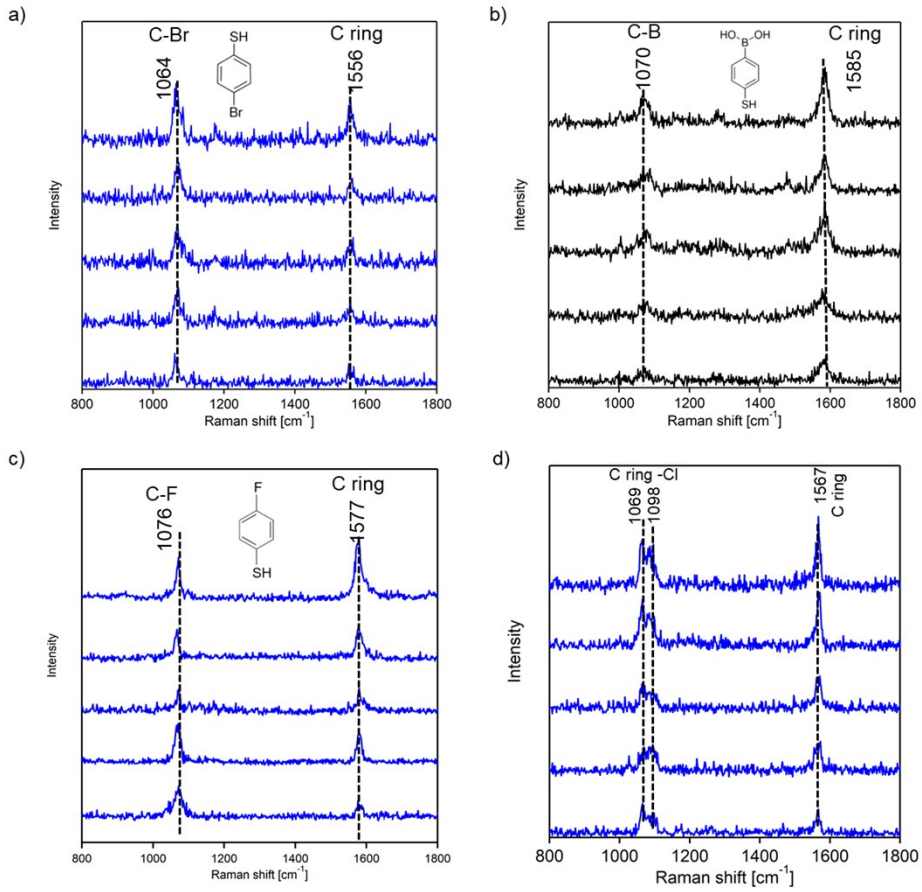

Fig. S6 More TERS spectra of (a) 4-BTP, (b) 4-MPBA, (c) 4-FTP and (d) 4-CTP.

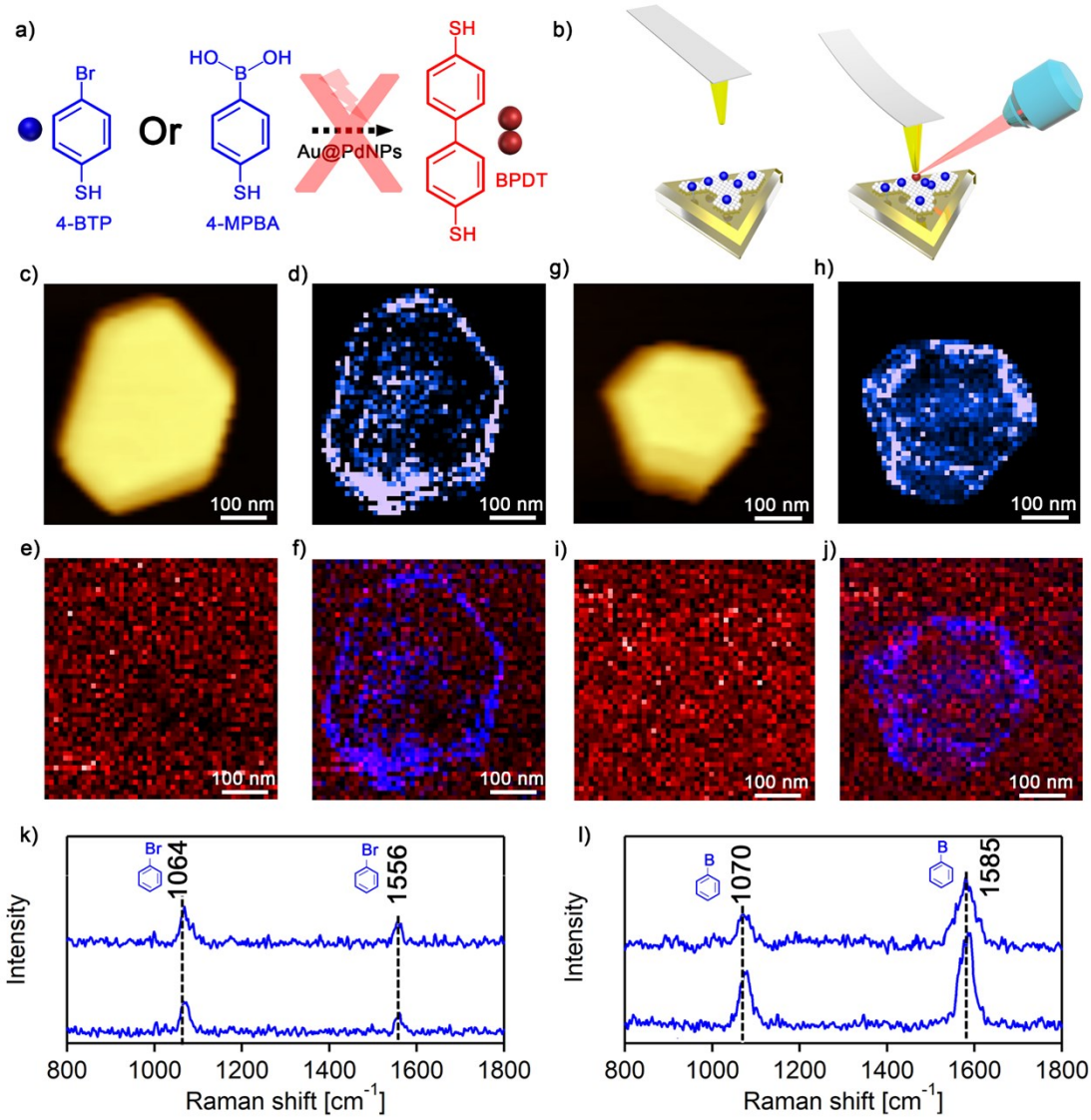

Fig. S7. (a) Reaction equation between 4-BTP and 4-MPBA on Au@PdNPs. (b) Illustration for the reaction before and after the coupling took place by TERS. (c) In-situ AFM image of 4-BTP-modified Au@PdNPs made by unmodified Au-coated tip. (d-e) TERS image of Au@PdNPs (10 nm per pixel) acquired with a modified tip with 4-BTP. Intensity of 1064 cm^{-1} band (C_{ring} -bromo vibration) of 4-BTP is shown in blue, intensities of 1593 cm^{-1} (C_{ring} - C_{ring}) of BPDT is shown in red, the red spots in (e) only show background where no identical bands was found at 1593 cm^{-1}. (f) Overlapping TERS image of 4-BTP and BPDT that evident no existence of BPDT. (l) Typical SERS spectra proved the successful modification of 4-MPBA on TERS tip. (g) In-situ AFM image for TERS on 4-MPBA with unmodified Au-coated tip. (h-i) TERS image of Au@PdNPs (10 nm per pixel) modified with 4-MPBA. Intensity of 1070 cm^{-1} band (C_{ring} -boron vibration) of 4-MPBA is shown in blue, intensities of 1593 cm^{-1} (C_{ring} - C_{ring}) of BPDT is shown in red. (j) Overlapping TERS image of 4-MPBA and BPDT shows no existence of BPDT. (k-l) Typical TERS spectra extracted from chemical maps on Au@PdNPs (d, h) showing presence of 4-BTP and 4-MPBA.

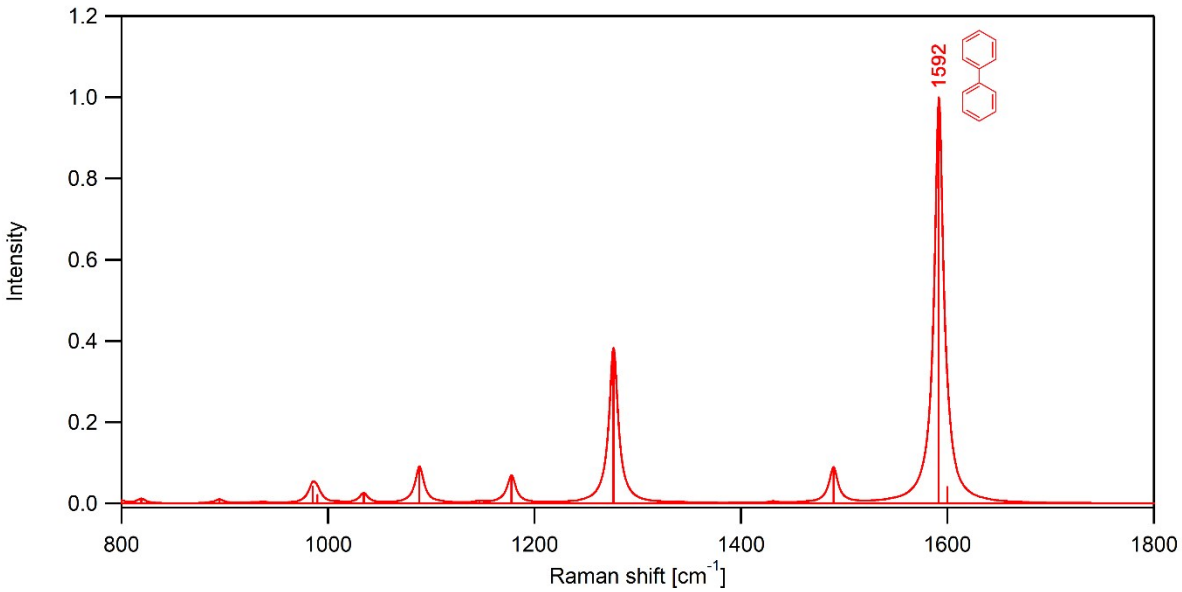

Fig. S8. Raman spectrum of Biphenyl (BP) obtained from DFT calculations.

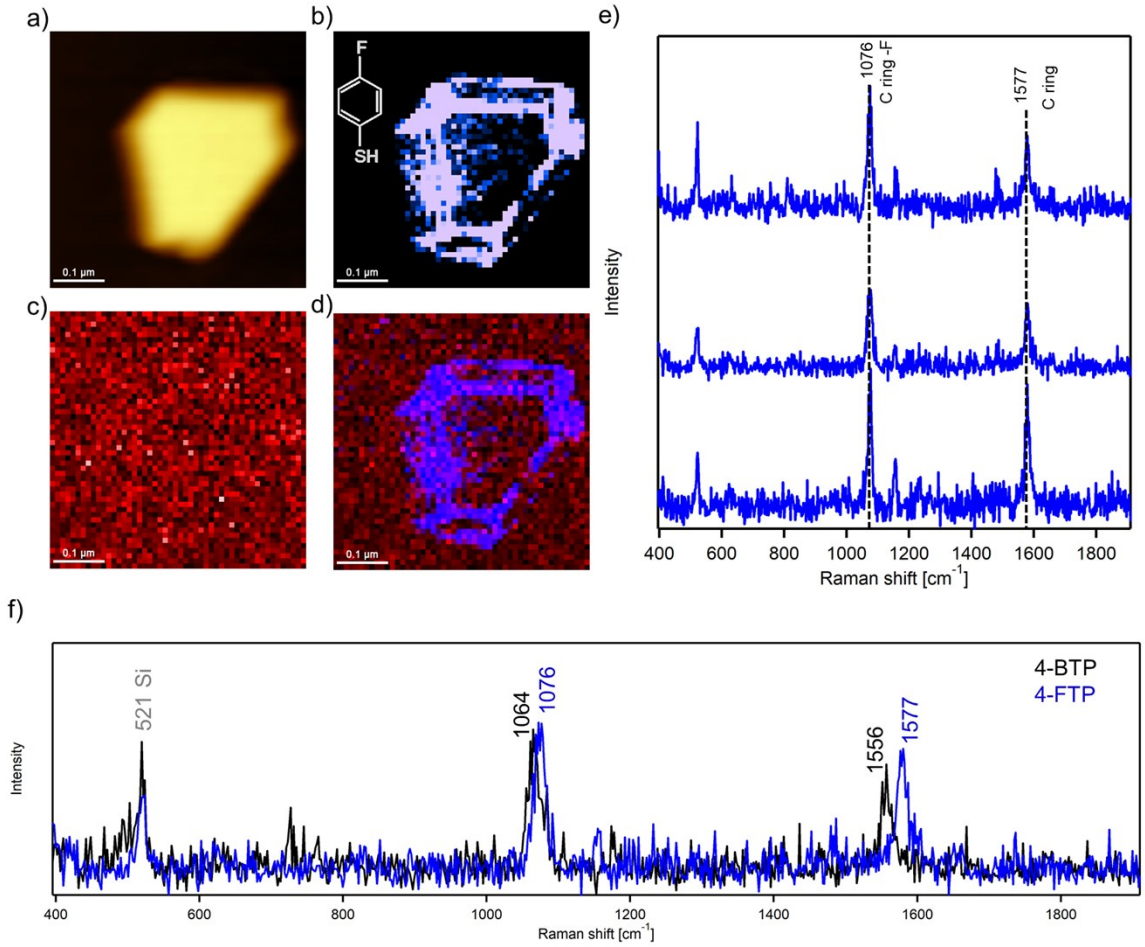

Fig. S9. TERS imaging of 4-FTP with non-modified Au-coated tip. (a) In-situ AFM image of Au@PdNPs with a monolayer of 4-FTP made with unmodified Au-coated tip. (b-c) TERS images of 4-FTP on Au@PdNPs. (c-d) Intensity of 1076 cm^{-1} band (C_{ring} - Fluoro vibration) of 4-FTP is shown in blue, intensities of 1593 cm^{-1} (C_{ring} - C_{ring}) of BPDT is shown in red, the red spots in (c) only show background where no identical bands were found at 1593 cm^{-1}. (d) Overlapping TERS image of 4-FTP and BPDT that evident lack of BPDT on the surface of Au@PdNPs. (e) Typical spectra extracted from the TERS image of Au@PdNPs (b) showing formation of 4-FTP. (f) Overlapping TERS spectra of 4-FTP and 4-BTP showing the different vibrational fingerprint of these two molecules.

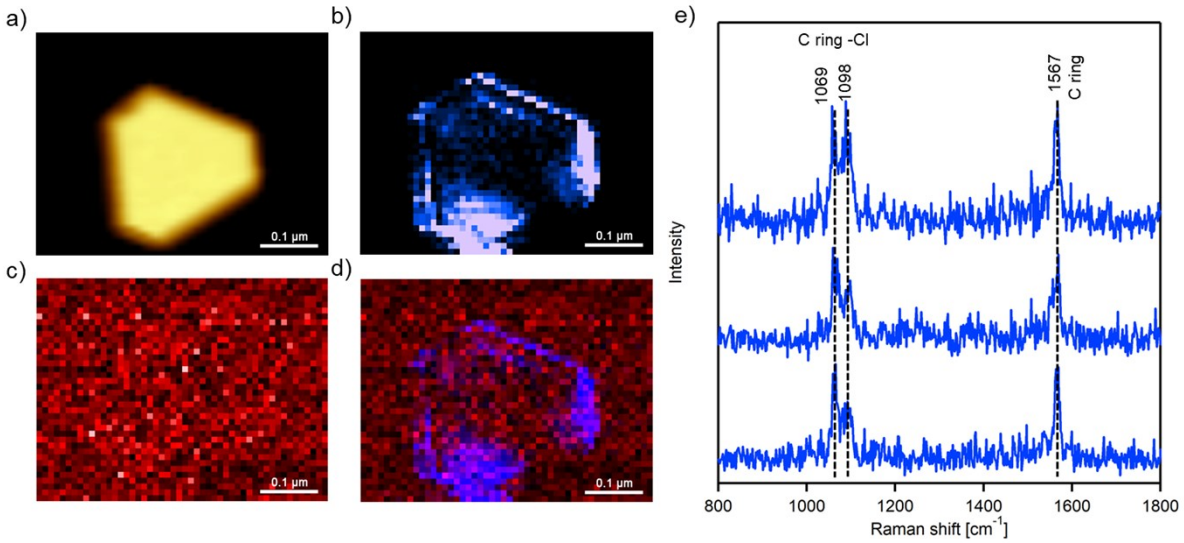

Fig. S10. TERS imaging of 4-CTP with non-modified gold-coated tip. (a) In-situ AFM image of Au@PdNPs with a monolayer of 4-CTP acquired with unmodified Au-coated tip. (b-c) TERS images of 4-CTP on Au@PdNPs. (c-d) Intensity of 1069 and 1098 cm^{-1} bands (C_{ring} - chloro vibration) of 4-CTP is shown in blue, intensities of 1593 cm^{-1} (C_{ring} - C_{ring}) of BPDT is shown in red, the red spots in (c) only show background where no identical bands were found at 1593 cm^{-1}. (d) Overlapping TERS image of 4-CTP and BPDT that evident the lack of BPDT formation. (e) Typical spectra extracted from TERS image (b) of Au@PdNPs showing formation of 4-CTP.

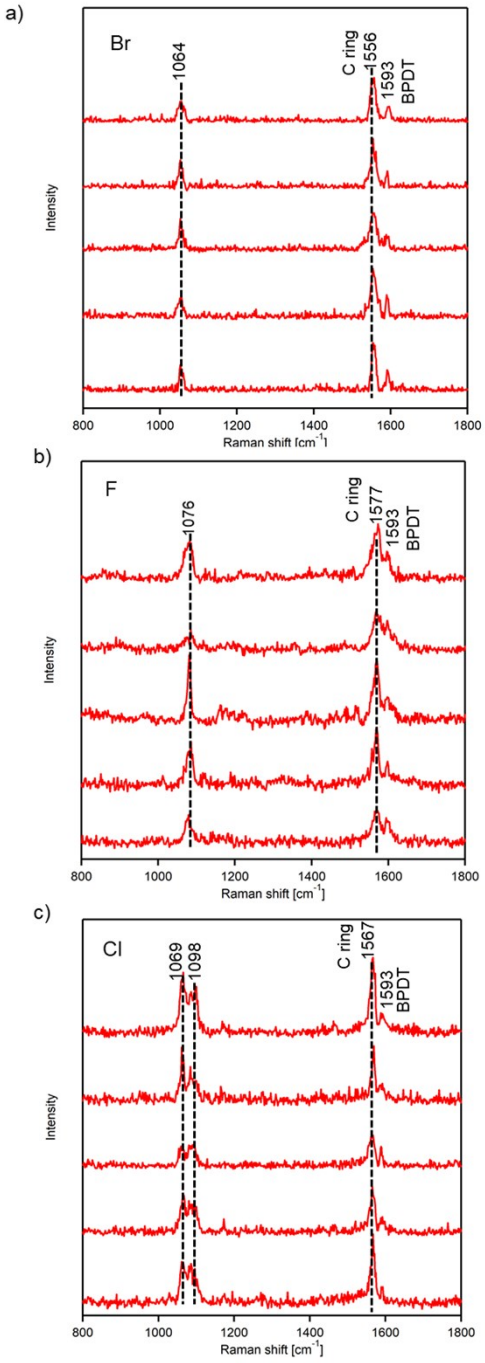

Fig. S11 TERS spectra of BPDT yield from (a) 4-BTP, (b) 4-FTP and (c) 4-CTP.

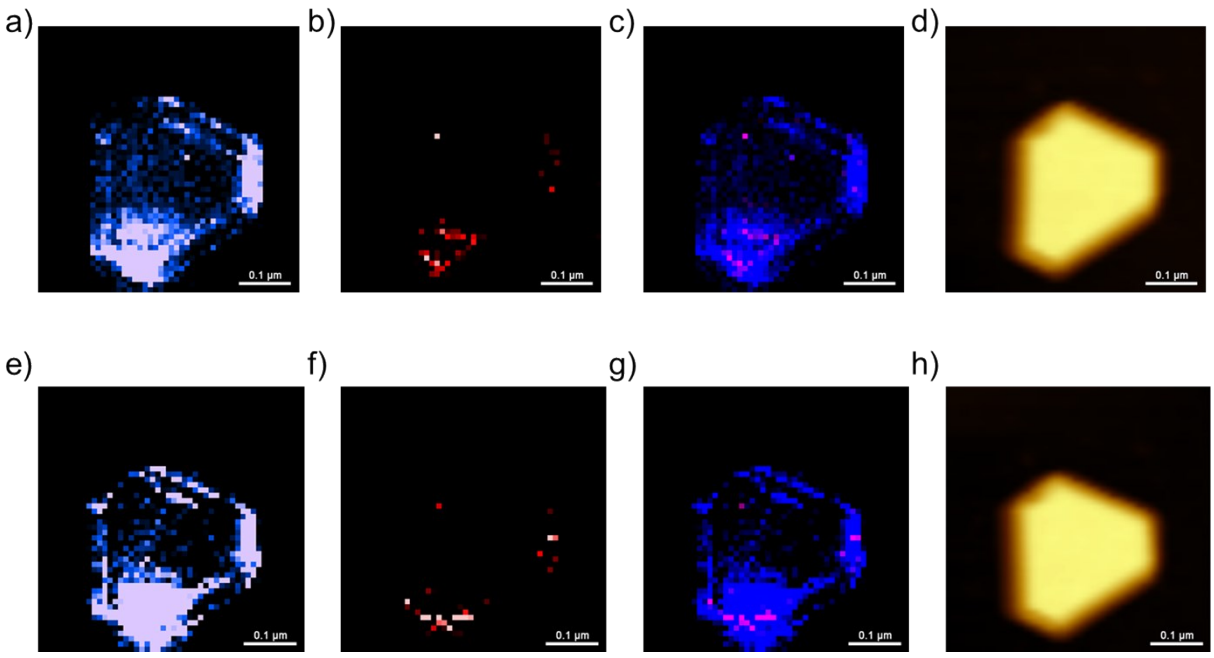

Fig. S12. TERS imaging of the product with a second non-modified Au-coated tip. (a-c) TERS images of 4-CTP on the surface of Au@PdNPs made with 4-MPBA modified Au-coated tip. (d) Corresponding AFM image of the Au@PdNPs. (e-g) New round of TERS imaging of Au@PdNPs after the previous round of TERS imaging (a-c) with a non-modified Au-coated tip. (h) Corresponding AFM image of the Au@PdNPs. Intensity of 1069 and 1098 cm^{-1} band (C_{ring} - chloro vibration) of 4-CTP is shown in blue, intensities of 1593 cm^{-1} (C_{ring} - C_{ring}) of BPDT is shown in red.

Table S1. Catalytic sites and yield of BPDT with different 4-XTP (X=F, Cl, Br) and 4-MPBA as reactants.

Tip	Au@PdNPs	Catalytic sites/total	Yield
4-MPBA	4-FTP	86/4599	1.87 %
4-FTP	4-MPBA	47/2784	1.69 %
4-MPBA	4-CTP	58/1648	3.52 %
4-CTP	4-MPBA	39/1025	3.80 %
4-MPBA	4-BTP	72/1457	4.94 %
4-BTP	4-MPBA	110/2152	5.11 %

References

[1] Li, Z.; Rigor, J.; Large, N.; El-Khoury, P.; Kurouski, D., J. Phys. Chem. C 2021, 125, 2492–2501.

[2] E. Apra, E. J. Bylaska, W. A. de Jong, N. Govind, K. Kowalski, T. P. Straatsma, M. Valiev, H. J. J. van Dam, Y. Alexeev, J. Anchell, V. Anisimov, F. W. Aquino, R. Atta-Fynn, J. Autschbach, N. P. Bauman, J. C. Becca, D. E. Bernholdt, K. Bhaskaran-Nair, S. Bogatko, P. Borowski, J. Boschen, J. Brabec, A. Bruner, E. Cauet, Y. Chen, G. N. Chuev, C. J. Cramer, J. Daily, M. J. O. Deegan, T. H. Dunning Jr., M. Dupuis, K. G. Dyall, G. I. Fann, S. A. Fischer, A. Fonari, H. Fruchtl, L. Gagliardi, J. Garza, N. Gawande, S. Ghosh, K. Glaesemann, A. W. Gotz, J. Hammond, V. Helms, E. D. Hermes, K. Hirao, S. Hirata, M. Jacquelin, L. Jensen, B. G. Johnson, H. Jonsson, R. A. Kendall, M. Klemm, R. Kobayashi, V. Konkov, S. Krishnamoorthy, M. Krishnan, Z. Lin, R. D. Lins, R. J. Littlefield, A. J. Logsdail, K. Lopata, W. Ma, A. V. Marenich, J. Martin Del Campo, D. Mejia-Rodriguez, J. E. Moore, J. M. Mullin, T. Nakajima, D. R. Nascimento, J. A. Nichols, P. J. Nichols, J. Nieplocha, A. Otero-de-la-Roza, B. Palmer, A. Panyala, T. Pirojsirikul, B. Peng, R. Peverati, J. Pittner, L. Pollack, R. M. Richard, P. Sadayappan, G. C. Schatz, W. A. Shelton, D. W. Silverstein, D. M. A. Smith, T. A. Soares, D. Song, M. Swart, H. L. Taylor, G. S. Thomas, V. Tipparaju, D. G. Truhlar, K. Tsemekhman, T. Van Voorhis, A. Vazquez-Mayagoitia, P. Verma, O. Villa, A. Vishnu, K. D. Vogiatzis, D. Wang, J. H. Weare, M. J. Williamson, T. L. Windus, K. Wolinski, A. T. Wong, Q. Wu, C. Yang, Q. Yu, M. Zacharias, Z. Zhang, Y. Zhao, R. J. Harrison, *J Chem. Phys.* 2020; 152, 184102.

[3] J. P. Perdew, K. Burke, M. Ernzerhof, *Phys. Rev. Lett.* 1996; 77, 3865-3868.

[4] F. Weigend, R. Ahlrichs, *Phys. Chem. Chem. Phys.* 2005; 7, 3297-3305.

[5] F. Weigend, *Phys. Chem. Chem. Phys.* 2006; 8, 1057-1065.

[6] M. Cardona, G. Guntherodt, *Topics in Applied Physics* 1982; 50, 1-18.

[7] W. F. Murphy, W. Holzer, H. J. Bernstein, *Applied Spectroscopy* 1969; 23, 211.